Desalination and Water Treatment
www.deswater.com
51 (2013) 1690–1699
February
1944-3994/1944-3986
doi: 10.1080/19443994.2012.693676
Taylor & Francis
Taylor & Francis Group

Biosorption of lead from aqueous solution by biologically activated date pedicels: batch and column study

H. Yazid*, L. Amour, A. Terkmani, R. Maachi

Laboratory of Reaction Engineering, Faculty of Mechanical and Processes Engineering, University of Sciences and Technology Houari Boumediene, BP 32 El Alia, Bab Ezzouar, 16111 Algiers, Algeria
Tel./Fax: +213 21 24 79 19; email: yazhyn1@yahoo.fr

Received 28 March 2012; Accepted 10 May 2012

ABSTRACT

Biosorption of lead by biologically activated date pedicels using a batch system and a continuous up-flow fixed bed column was studied. Batch experiments were conducted to determine the biosorption capacity, equilibrium time and optimal pH. The maximum biosorption capacity of lead was 11.56 $mg\,g^{-1}$ at an optimal pH of 5.2. The Langmuir and Freundlich models were used to explain the equilibrium data. The Langmuir model showed a better fit of data with a correlation coefficient of 0.999. The kinetics of biosorption followed pseudo-second-order model. For continuous biosorption experiments, breakthrough curves were analyzed at different flow rates and porosities of the pedicels' bed. Breakthrough time, time of saturation, fractional capacity and the optimal area of operation were determined. We concluded that biosorption is favored for its lower rate and porosity.

Keywords: Lead; Biosorption; Kinetic study; Equilibrium isotherm; Fixed bed; Mass transfer zone

1. Introduction

Pollution of the environment by heavy metals such as lead, mercury and cadmium is a serious problem because of their toxic effects on human health and other living organisms [1]. These heavy metal ions cannot be biodegraded; hence they easily accumulate in the human body and cause various diseases. Lead (Pb(II)) is a heavy metal that is commonly present in different types of industrial effluents and is responsible for environmental pollution, toxicity and heavy metal contamination. The toxicological effects of Pb in humans include inhibition of hemoglobin formation (anemia), sterility, hypertension, learning disabilities, abortion, kidney damage and mental retardation [2–4]. Thus, the removal of lead from water is essential. Many physicochemical strategies, such as filtration, chemical precipitation, electrochemical treatment, ion exchange, oxidation or reduction, reverse osmosis, and evaporation recovery, have been developed to remove heavy metals, including lead, from polluted water [5–8]. However, there are some disadvantages for traditional physicochemical methods to treat lead-polluted wastewater, such as expensive cost, low efficiency, labor-intensiveness and lack of selectivity in the treating process [9,10]. Compared with the con-

*Corresponding author.

Presented at the International Conference on Desalination for the Environment, Clean Water and Energy, European Desalination Society, 23–26 April 2012, Barcelona, Spain

ventional methods, biosorption is considered to be a promising option to solve the environmental pollution of heavy metals. The major advantages of biosorption include low cost, high efficiency in removing heavy metals from diluted solutions, regeneration of the biosorbent and the possibility of metal recovery [10]. The promising challenge to traditional operation attracts people to exploit more bioresources as biosorbent in this research field. One of the main agricultural wastes in Algeria is pedicels of dates [11,12]. Targeting effective and inexpensive biomaterials for the elimination of metal wastes, biologically activated date pedicels (ASP) were investigated as a sorbent for lead by batch and column method.

The influences of various operating parameters such as contact time, initial metal concentration, biosorbent dose and initial pH of solution were investigated. The Langmuir and Freundlich models were used to fit the equilibrium isotherms. We apply the concept of the mass transfer zone (MTZ) [13] that helps to obtain the evolutions of the operating parameters of the fixed-bed at different flow rates and porosity of the pedicels' bed.

2. Materials and methods

2.1. Preparation of ADP

The dates' pedicels are by-products of the palm-tree date. The quantity of date stems produced in the South of Algeria is 9,200 tons per year; considering the units of transformation and the conditioning of dates in the South of Algeria, this is a significant volume of waste organic materials likely to be valued.

A part of crushed raw dates' pedicels (RDP) was put in static conditions in nitrate-enriched solution, and activated sludge sample was obtained from the aeration tank in the urban waste water treatment plant of the town of Ain El Benian (Algiers), with a daily renewed environment; this device enabled to enhance the development of denitrifying microorganisms already existing in activated sludge. Considering nitrates as acceptors of electrons and the dates' pedicels as a donor of electrons and as a potential carbon source to promote and stimulate the denitrification process, it is necessary that the organic matter contribution was sufficient for complete denitrification. If the organic matter became limiting, the efficiency of the denitrification decreased. The dates' pedicels were filtered; it was next washed with distilled water and dried at 60°C for 48 h. This pretreatment would allow the consumption of dissolved organic matter and the appearance of a bacterial film at the surface of the dates' pedicel particles.

2.2. FTIR study and surface area analysis

Fourier Transform Infrared (PerkinElmer FT-IR System 2000 Model) analysis was done on RDP and ADP to determine the surface functional groups that might be involved in lead(II) ions' sorption, and the spectra were recorded from 4000 to 400 cm^{-1}. The surface area of RDP and ADP was determined by Brunauer, Emett and Teller method using AS1-CT-9 (Quantachrome, USA) instrument by nitrogen adsorption–desorption measurements.

2.3. Preparation of the metal solution

Stock lead(II) solution was prepared by dissolving lead nitrate [$Pd(NO_3)_2$] in distilled water. Fresh dilutions were used for each set of experiments. pH of the used solutions was adjusted to the desired value by adding a slight quantity of solution HNO_3 or NaOH.

2.4. Batch biosorption studies

In order to assess and compare the sorption capacities of biosorbant RDP and ADP, the batch sorption experiments were conducted with 10 g L^{-1} of RDP and ADP in Erlenmeyer flasks. Biosorbent was added to 100 mL of lead solution (100 mg L^{-1}), and then the reaction mixture was agitated at 600 rpm. The effect of contact time on biosorption was investigated in the time range of 5–120 min. To determine the optimal lead(II) biosorption conditions, experiments were conducted with ADP. The effect of pH solution on the biosorption capacity for lead(II) was investigated at several pH values (2.3, 3.2, 3.9, 5.2 and 5.9) using a volume of 100 mg L^{-1} lead(II) solutions.

The effect of biosorbent concentration was studied in the concentration range of 2.5–30 g L^{-1}. The final reaction mixtures were filtered out and analyzed as per their metal ion concentrations using an atomic absorption spectrophotometer (SOLAAR, M6-GF95) with an air–acetylene flame. The instrument calibration was periodically checked (every 10 readings) using standard metal solutions. The amount of adsorption at equilibrium, q_e (mg g^{-1}) and q_t (mg g^{-1}) at time t, was given by the following relations:

$$q_e = \frac{(C_0 - C_e)V}{m} \quad (1)$$

$$q_t = \frac{(C_0 - C_t)V}{m} \quad (2)$$

where C_0, C_e and C_t (mg L^{-1}) are the liquid-phase concentrations of lead(II) ions initially, at equilibrium and at a given time t, respectively, V is the volume of solution (L) and m is the mass of biosorbent used (g).

The percentage of biosorbed lead ion was determined from the following equation:

$$R_e(\%) = \frac{(C_0 - C_e)100}{C_0} \quad (3)$$

2.5. Fixed-bed-column experiments

Continuous-flow biosorption experiments were conducted in glass column of 2 cm inner diameter and 40 cm in height. The column was packed with 5 g of immobilized ADP biomass to yield a bed height of 10 cm. A calming section of glass beads is placed at the bottom of the column, and another quantity of beads is placed above the bed of pedicels of dates to minimize the swelling of the bed and to prevent the biosorbent particles to be entrained by the upward flow of water. Lead solution of 100 mg L^{-1} was pumped to the top of the column, at flow rates of 2.77, 5 and 7.5 mL min^{-1}, using a peristaltic pump.

To study the effect of compaction of the bed on the breakthrough curve, 5 g of ADP was used for column packing. After each addition of a gram, several taps are typed at the bed surface using a glass rod to compact the material and homogenize the bed. The tests were carried out for an initial concentration of Pb(II) ions of 100 mg L^{-1}, a pH of 5.2 and a flow rate of 5 mL min^{-1}. Samples were collected from the exit of the column at regular time intervals and analyzed for residual lead concentrations.

We apply the concept of the MTZ that helps to obtain the evolutions of the operating parameters of the fixed bed. This concept was developed by Mickaels [14] for ionic exchange and applied by Luchkis [15] for the adsorption. The MTZ is the portion of the filter where major adsorption occurs, where adsorbate is actively removed from the liquid phase at any given moment. Three characteristics determine the MTZ, noticing that these characteristics can be calculated in referring to either the solid or the liquid phases [13].

The fractional capacity is given by the ratio:

$$F = \frac{\int_{V_p}^{V_s}(C_0 - C_t)dV}{C_0(V_s - V_p)} \quad (4)$$

F is defined by the ratio of the quantity of biosorbant that really participates in transfer process to the total quantity of biosorbant used by the height of the MTZ.

V_s is the volume of effluent treated whose instantaneous concentration C_t at the exhaustion time t_s is equal to or more than 80% of the initial concentration C_0. This concentration is chosen arbitrarily depending on the working mode of the filter, from economic point of view.

V_p is the volume of effluent treated whose the instantaneous concentration C_p at the breakthrough time t_p is <5% of the initial concentration.

The height of the MTZ, H_Z is the area where the entire phenomenon of adsorption practically takes place, which is calculated as follows:

$$H_Z = \frac{Z(V_s - V_p)}{V_p + F(V_s - V_p)} \quad (5)$$

where Z is height of the bed (cm)

The rate of the movement of the MTZ permits the calculation of rate of bed saturation. It is directly related to the height of MTZ. The smaller the depth of MTZ, the quicker the rate of transfer and more rapid the saturation of the bed. It is given as follows:

$$U_Z = \frac{Q \cdot H}{V_p + F(V_s - V_p)} \quad (6)$$

where U_Z is the rate of movement of MTZ (cm min^{-1}) and Q is the volumetric flow (mL min^{-1}).

3. Results and discussion

3.1. Characterization of RDP and ADP

Some chemical and physical characteristic features of RDP and ADP such as mean diameter, bulk density, pH_{pzc} and surface area are listed in Table 1.

Table 1
Physical and chemical characteristics of raw and biological activated pedicels of dates

	Mean diameter (μm)	Bulk density (g/cm^3)	Point of zero charge $pH_{(pzc)}$	Surface area (m^2/g)
RDP	225	0.45	5.6	2.94
ADP	290	0.32	6.7	0.08

The point of zero charge (pH_{pzc}), corresponding to the point of balance between positive and negative charges on the material surface, was determined according to the experimental procedure described by Mishra and colleagues [16].

Dates' pedicels present a low surface area, which decreased after biological treatment; it decreased from 2.94 to 0.08 $m^2 g^{-1}$, most likely due to the filling of pores by bacteria formed during the biological treatment. pH_{pzc} increased from 5.6 to 6.7, due to the formation of basic functions on the surface of dates' pedicels after biological treatment, which suggests operating conditions more favorable for metal ion binding.

The FTIR spectra of RDP and ADP (Fig. 1) display a number of absorption peaks indicating the presence of different functional groups and reflecting the complex nature of the biomass. The FTIR spectra of RDP display a wide absorption peak at 3,447 cm^{-1}, assigned to the stretching of O–H group due to inter- and intramolecular hydrogen bonding of polymeric compounds (macromolecular associations), such as alcohols, phenols and carboxylic acids, as in cellulose and lignin. The O–H stretching vibrations occurred within a broad range of frequencies, indicating the

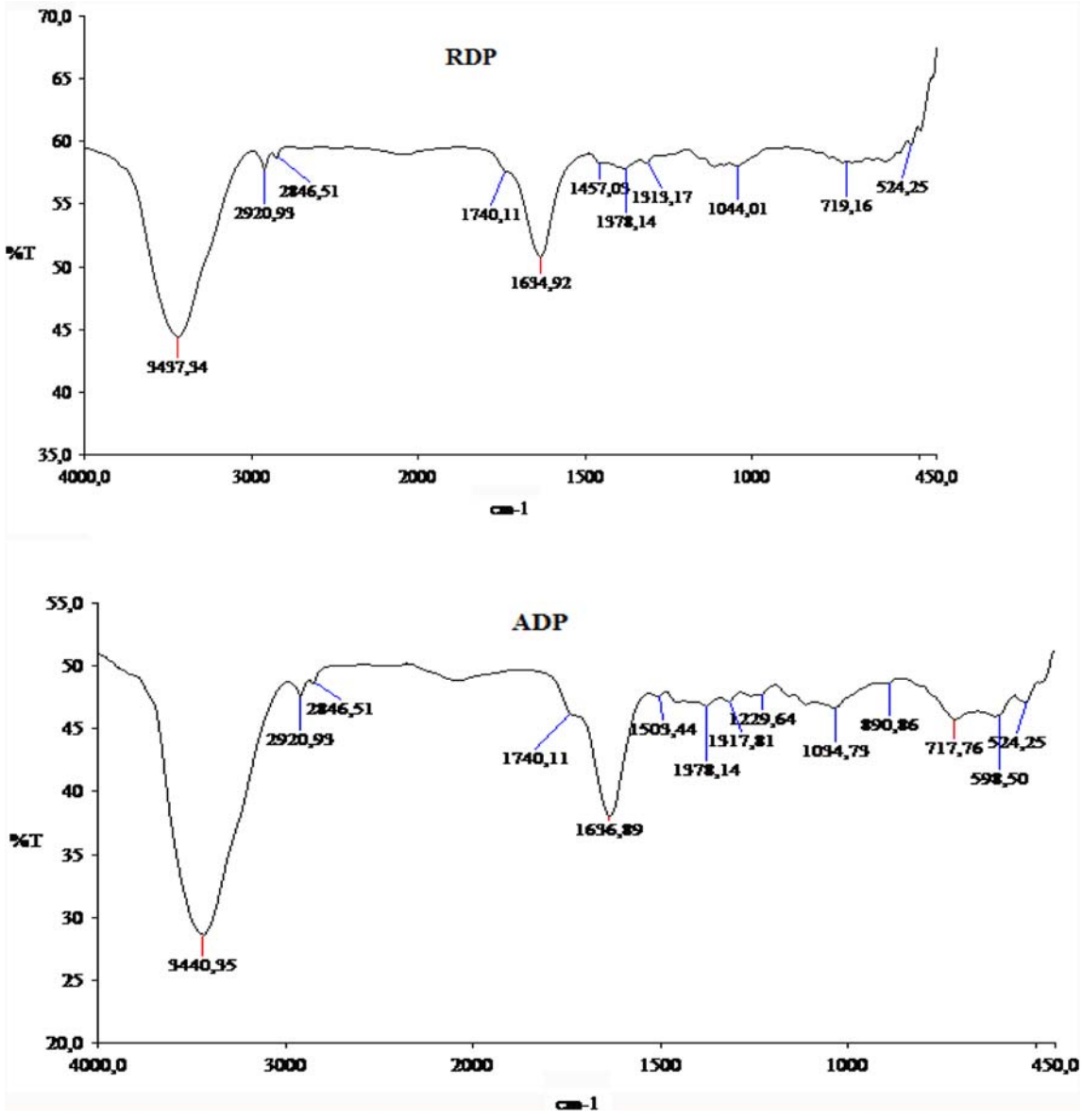

Fig. 1. FTIR spectra of RDP and ADP.

presence of hydroxyl groups and bonded O–H bands of carboxylic acids. The band of 2,919 cm^{-1} was stretching vibration of C–H, and the absorption peak at 1,736 cm^{-1} was assigned as unconjugated carbonyl vibration. Asymmetric and symmetric stretching vibrations of ionic carboxylic groups ($–COO^-$) appeared at 1,634 and 1,409 cm^{-1}, respectively. The absorption peak at 1,245 cm^{-1} was assigned to C–O stretching vibration. The peaks were observed at 1,071 cm^{-1} corresponding to stretching vibration of O–H of polysaccharides [17–19]. Therefore the FTIR spectrum of RDP clearly showed the presence of carboxyl and hydroxyl groups in abundance. In biopolymers, these groups may act as proton donors; hence, deprotonated hydroxyl and carboxyl groups may be involved in coordination with metal ions.

It can be seen from the FTIR spectrum of ADP that some peaks disappeared and new peaks are observed after biological treatment. The latter can cause degradation of the organic matter, consisting mainly of cellulose, which constitutes the intercellular walls, and the deposit of bacterial film, which has been yielded during the biological pretreatment, can introduce some new functional groups.

3.2. Biosorption conventional experimental batch studies

In this section, the effect of different experimental variables like contact time, pH and biosorbent dosage, which are conventionally being used to optimize the experimental conditions for the maximum metal uptake by ADP, is described comprehensively.

3.2.1. Effect of the contact time

Fig. 2 shows that the amount of metal ion biosorbed increased with the contact time. The biosorption of lead(II) was fast for the first 5 min for RDP and ADP, as a result of the free binding sites on the biomass. The biosorption equilibrium was achieved within 60 min, and the percentages of lead(II) ion biosorbed were 74 and 91.5% with RDP and ADP, respectively. The biological pretreatment of the dates' pedicels enhanced their biosorption capacity, although the surface area of dates' pedicels decreased after biological treatment. Furthermore, work on a variety of microorganisms has clearly shown that bacteria excreting extracellular polysaccharides have high metal adsorption potential [20].

3.2.2. Effect of the initial pH

pH is the major parameter controlling metal sorption processes. As seen in Fig. 3, lead(II) sorption on ADP was drastically reduced by decreasing the solution pH. Maximum lead(II) sorption (99.4%) occurred at pH 5.2, and lead(II) was very slightly sorbed at pH 2.3. Lead found in its free form Pb^{2+} at low pH values (<3.5), the first hydrolysis $PbOH^+$, more easily adsorbed, appears at this pH. The minimal sorption amount obtained at low pH was partly due to the fact that protons were strong competing sorbate, because of their higher concentration and high mobility, and partly due to the fact that the solution pH influenced the sorbent surface charge. The surface charge of ADP was positive at pH < PZC = 6.7, neutral at pH = PZC and negative at pH > PZC. For decreasing acidity in the solution, the deprotonation of acid functional groups, such as carboxyl amine and hydroxyl, was strengthened and the attraction increased between negative charge on biomass and positive metal cations [21].

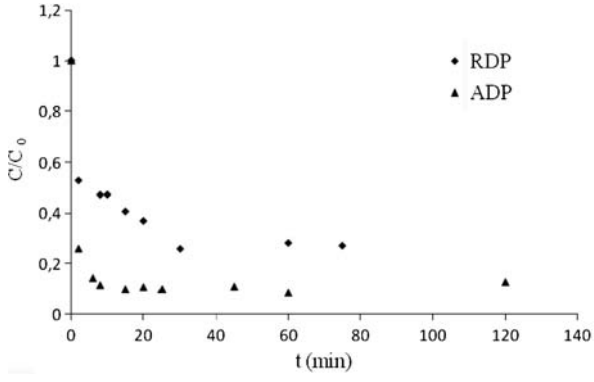

Fig. 2. Effect of contact time on biosorption of lead(II) by RDP and ADP. pH = 5.2, $C_0 = 100\ mg\ L^{-1}$, $m = 10\ g\ L^{-1}$ and $T = 22$°C.

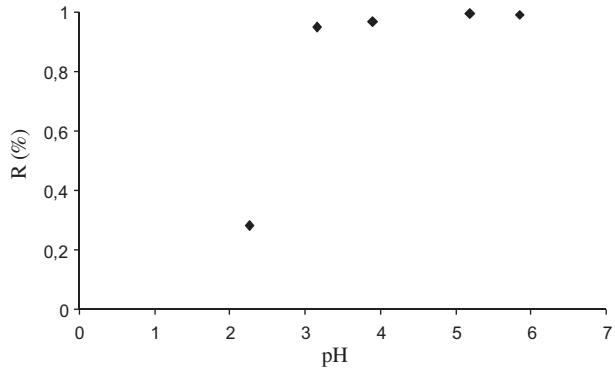

Fig. 3. Effect of initial pH on the biosorption of lead(II) by ADP: contact time 60 min, $m = 25\ g\ L^{-1}$, $C_0 = 100\ mg\ L^{-1}$ and $T = 24$°C.

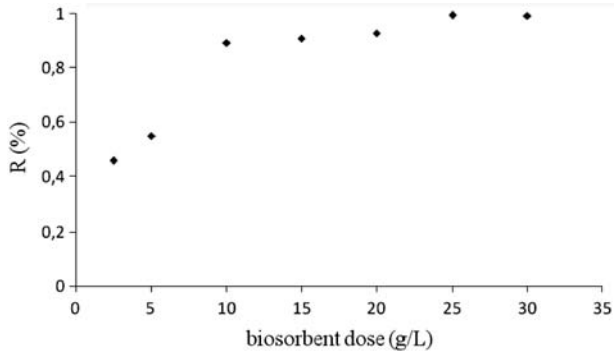

Fig. 4. Effect of biosorbent dose on the rate of biosorption of lead(II) by ADP: contact time = 90 min, pH = 5.2, $C_0 = 100\,mg\,L^{-1}$ and $T = 22$°C.

3.2.3. Effect of the biosorbent dosage:

Biosorbent dosage allows to determine the biosorbent capacity for a given initial concentration of metal ion. Fig. 4 shows a sharp increase in the biosorption yield for biosorbent dosage, increasing from 2.5 to $30\,g\,L^{-1}$. The lead(II) biosorption rate onto ADP increased from 47.7 to 99.3% with the increase in biosorbent dosage from 2.5 to $25\,g\,L^{-1}$. The observed enhancement in lead(II) biosorption yield for increasing biosorbent concentration could be the consequence of an increase in the number of possible binding sites and surface area of the biosorbent [22]. The obtained results also showed that there was a slight increase in percentages of lead(II) removal when adsorbent dose increased beyond $10\,g\,L^{-1}$. This suggests that after a certain dose of biosorbent, the maximum biosorption will be attained, and hence, the number of ions remains nearly constant even for further incrementation of biosorbant dosage.

3.3. Data analysis

Data analysis for biosorption kinetics was carried out by considering the pseudo-second-order model, and the well-known Langmuir and Freundlich adsorption isotherms models were considered for equilibrium study.

3.3.1. Kinetic study

In batch systems, adsorption kinetic is described by a number of models based on adsorption equilibrium such as the pseudo-second-order. The predicted values are validated by the correlation coefficient r^2 and the graphical analysis.

The linearized pseudo-second-order kinetic model takes the following form [23,24]:

$$\frac{t}{q_t} = \frac{1}{k_2 q_e^2} + \frac{t}{q_e} \quad (7)$$

where q_t and q_e are the amounts of metal adsorbed at a given time t and at equilibrium, respectively and k_2 ($g\,mg^{-1}\,min^{-1}$) is the second-order reaction rate constant.

A straight line plot of t vs. t/q_t with a correlation coefficient of 0.99 (Fig. 5), showed the validity of pseudo-second-order model. The applicability of pseudo-second-order kinetics model suggested that the lead biosorption to ADP was based on chemical reaction, involving the exchange of electrons between biosorbent and metal [25]. The reaction rate constant k_2 and equilibrium biosorption capacity q_e were determined from the slope and intercept of the straight line plot, which were, respectively, $0.65\,g\,mg^{-1}\,min^{-1}$ and $8.36\,mg\,g^{-1}$. The value of equilibrium capacity is in close agreement with $8.4\,mg\,g^{-1}$ determined experimentally.

3.3.2. Isotherm modeling

The adsorption phenomena at the solid–liquid interface were commonly described by adsorption isotherm models, which are essential data source for the practical design of adsorption systems and understanding the relation between adsorbent and adsorbate [18].

The sorbent was set in contact with various concentrations (50–500 $mg\,L^{-1}$) of lead(II) solutions at pH 5.2 until equilibrium was achieved. Metal-removing capacity of ADP for the metal increased with an increase in metal ion concentrations until reaching a maximum capacity (Fig. 6). To examine the relationship between the metal sorption capacity (q_e) and the

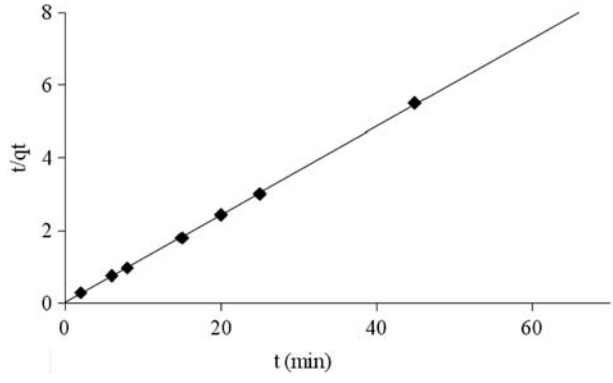

Fig. 5. Application of pseudo-second-order model. pH = 5.2, $C_0 = 100\,mg\,L^{-1}$, $m = 10\,g\,L^{-1}$ and $T = 22$°C.

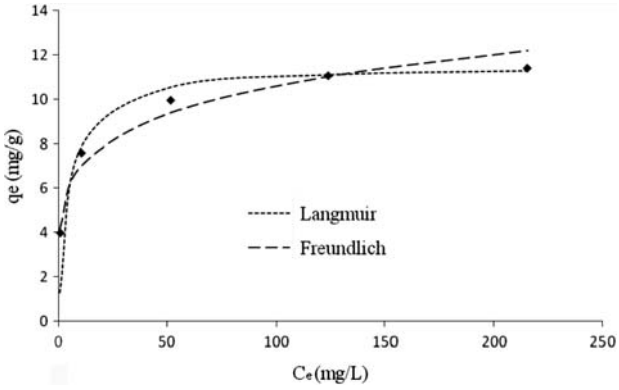

Fig. 6. Experimental and adjusted isotherms for biosorption of lead(II) by ADP. $T = 26$°C, pH = 5.2 and $m = 25\,g\,L^{-1}$.

concentration of metal ions at equilibrium (C_e), the sorption equilibrium data were fit to Langmuir and Freundlich isotherms models. These two models are widely used for adsorption data analysis since they have the ability to describe experimental results for a wide range of initial metal concentrations. Both isotherm models can be easily transformed into linear forms to obtain adjustable parameters by linear regression analysis [26].

The Langmuir isotherm theory relies on the chemical or physical interaction (or both) postulated to occur between the solute and the available vacant sites on the sorbent surface, which may be described by the linear form as follows:

$$\frac{1}{q_e} = \frac{1}{q_{max} b}\frac{1}{C_e} + \frac{1}{q_{max}} \quad (8)$$

where q_e is the amount of sorbate sorbed at equilibrium (mg g^{-1}), q_{max} is the maximum metal uptake capacity ($mg\,g^{-1}$), C_e is the equilibrium concentration ($mg\,L^{-1}$) and b ($L\,mg^{-1}$) is a coefficient related to the affinity between the metal ion and the sorbent.

The Freundlich isotherm is an empirical equation that is based on the sorption of a sorbate on a heterogeneous surface of a sorbent, as given by the following equation:

$$\mathrm{Ln}(q_e) = \mathrm{Ln}(K_F) + n\mathrm{Ln}(C_e) \quad (9)$$

where K_F and n are the Freundlich empirical constants indicative of sorption capacity and sorption intensity, respectively.

The Langmuir and Freundlich constants and the corresponding correlation coefficients (r^2) are given in Table 2. Lead biosorption obeyed a Langmuir model rather than a Freundlich model, since the correlation coefficients were 0.999 and 0.978, respectively. The values of $1/n$ were smaller than 1 (Table 2), indicating that the biosorption process was favorable in the considered conditions. The maximum biosorption capacity estimated using the Langmuir isotherm model was equal to $11.56\,mg\,g^{-1}$ (Table 2), above or equal to the values reported for natural biosorbents (Table 3).

3.4. Continuous biosorption in packed column

Batch biosorption studies provide information on biosorption equilibrium and kinetics. For practical applications of biosorption process, continuous-flow experiments are essential, and these are conducted in fixed bed columns. This type of arrangement makes efficient utilization of the concentration gradient between the metal biosorbed and its portion remaining in the solution. The overall performance of the column is judged by its service time, which is defined as the time until the biosorbed metal breaks through the column bed and is detected in the column effluent. At that time, column is considered to be saturated and must be regenerated. The column performance was studied by varying the flow rate, bed height or porosity.

3.4.1. Effect of flow rate

Flow rate is an important characteristic in evaluating the performance of biosorption, for continuous treatment of wastewater on industrial scale. The effect of flow rate on lead biosorption was studied by varying the flow rate from 2.77 to $7.5\,mL\,min^{-1}$, while the bed height and initial metal concentration were held constant at 10 cm and $100\,mg\,L^{-1}$, respectively. The experimental breakthrough curves are shown in Fig 7. The column performed well at the lowest flow rate. An earlier breakthrough and exhaustion times were achieved when the flow rate was increased from 2.77 to $7.5\,mL\,min^{-1}$. The column breakthrough time was

Table 2
Isotherm constants for lead(II) biosorption onto ADP

Langmuir constants			Freundlich constants		
q_{max} ($mg\,g^{-1}$)	b ($L\,mg^{-1}$)	r^2	K_f	$1/n$	r^2
11.56	0.204	0.999	4.57	0.183	0.978

Table 3
Comparison of biosorption capacity of ADP with those of various sorbents

Adsorbents	q_{max} (mg g^{-1})	References
Oryza sativa L. husk	8.6	[27]
Rice husk ash	12.6	[28]
Aspergilus niger	10.1	[29]
Olive pomace	7.0	[30]
Sawdust	12.6	[31]
Groundnut shells	12.2	[31]
Waste tea leaves	2.1	[32]
ADP	11.56	Present study

reduced from 5.25 to 2.5 h. This behavior was due to the decrease in the residence time, which restricted the contact of metal solution to the biosorbent. At higher flow rates, the metals ions did not have enough time to diffuse into the pores of the biosorbent, and they leave the column before equilibrium occurred. Due to this reason, column exhaustion time was reduced. This resulted in low metal uptake and least percentage removal at higher flow rates. As the flow rate increases, metal concentration in the effluent increased rapidly, resulting in sharper breakthrough curves. At lower flow rates, the residence time of the metal solution in the column was increased, and metal ions have more time to diffuse into the pores of biosorbent through intraparticle diffusion.

3.4.2. Effect of bed porosity

The uptake of metals in fixed bed column is dependent on the porosity of biosorbent in the column. The experiments were performed at three different bed heights of 7, 8.5 and 10 cm, achieved by packing 5 g immobilized ADP in the column. The flow rate and initial metal concentration were kept constant at 5 mL min^{-1} and 100 mg L^{-1}, respectively. As depicted by Fig. 8, the breakthrough time varied with bed porosity. The breakthrough time increased from 3.75 to 5.25 h with decreasing bed porosity, which corresponds to the reduction in the height of the bed depth from 10 to 7 cm. For high bed porosity, the axial dispersion phenomenon predominates in mass transfer and reduces the diffusion of metal ions. The metal ions do not have enough time to diffuse into the whole of the biosorbent mass, due to which reduction in breakthrough time occurred. With the decrease in bed porosity, the radial dispersion phenomenon predominates in mass transfer, allowing the metal ions to diffuse deeper inside the biosorbent.

The breakthrough curves obtained, the characteristics F, H_Z and U_Z, and their evolutions are determined as functions of the rate of flow and of the bed porosity (Table 4). These three parameters enable us to estimate the behavior of the filter and to understand how the process of adsorption is done and how to act for an improvement.

A variation in the flow rate does not affect (or slightly) the fractional capacity. A decrease in the bed porosity, which corresponds to the reduction in the height of the bed depth from 10 to 7 cm, is leading to an increase in the fractional capacity from 0.42 to 0.50.

We can study the height of the MTZ, $H_{Z,}$ and the number of units of transfer. H_Z is one of the most important parameters in adsorption column since it determines the elimination efficiency of the adsorbent

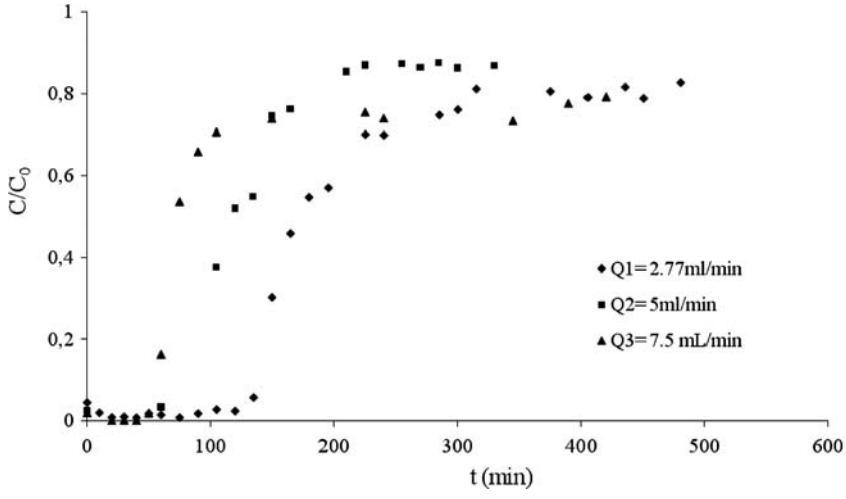

Fig. 7. Effect of flow rate on breakthrough curves.

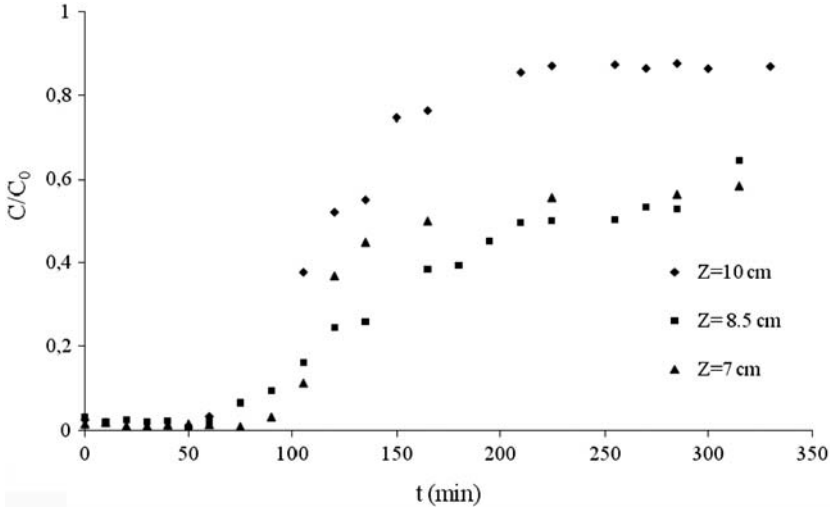

Fig. 8. Effect of bed porosity on breakthrough curves.

Table 4
Variation of the characteristics t_p, t_s, F, H_Z and U_Z with the rate of flow and the bed porosity

Q (mL min^{-1})	Z (cm)	t_p (min)	t_s (min)	F (–)	U_Z (cm min^{-1})	H_Z (cm)	H_Z/Z (–)
2.77	10	135	315	0.39	0.049	8.77	0.88
5	7	100	315	0.50	0.034	7.25	1.03
	8.5	70	315	0.39	0.051	12.58	1.48
	10	62	225	0.42	0.072	11.74	1.17
7.5	10	51	150	0.41	0.109	10.84	1.08

and the exchange rate between phases. The faster the exchange, the smaller the MTZ height, and more important the number of transfer units developed. An increase in the feed flow and/or the bed porosity leads to a decrease in the residence time of molecules in the column, due to the steric effect and/or the difficult choice of an adsorption site. For remedying this state, the MTZ increases its height, thereby offering more sites to the molecules, and compensates the resistance to the transfer by increasing its depth; in both cases, we have a reduction in the rate of mass transfer between the two phases.

On the contrary, decreasing the bed porosity, the radial dispersion phenomenon predominates in mass transfer and improves the diffusion of metal ions and the adsorption kinetic, as a result, an acceleration of the process.

Another characteristic of breakthrough curve, which is as important as the MTZ height, is its rate of the movement U_Z, which determines the working time of the filter. Increase in the volumetric flow, or the bed porosity, increases particularly the height of MTZ and, consequently, the rate of movement, thereby rapidly exhausting the ADP bed.

4. Conclusion

This study identified that ADP in free and immobilized forms could be used as potential sorbent for the removal of lead from wastewater. The biosorption has been found to be relatively fast. The maximum biosorption capacity of lead was 11.65 mg g^{-1} at pH 5.2. The pseudo-second-order and the Langmuir isotherm models were found to be the most appropriate to describe the kinetics and equilibrium of the biosorption process, respectively. The column breakthrough curves were analyzed at different flow rates and different bed porosities. The determining intrinsic parameters of the MTZ helped to explain the elimination efficacy and the variability of the biosorption phenomenon. The faster the adsorption mechanism, the smaller the height of MTZ and greater the number of transfer units. But in the dynamic adsorption, having a high NUT is not interesting, because exhaustion of

the bed occurs rapidly. Therefore, the optimal experimentation area is obtained at a lower flow rate ($2.77\,mL\,min^{-1}$) and at the lowest porosity of the ADP bed ($Z = 7\,cm$).

References

[1] D. Sud, G. Mahajan, M.P. Kaur, Agricultural waste material as potential adsorbent for sequestering heavy metal ions from aqueous solutions—a review, Biores. Technol. 99 (2008) 6017–6027.

[2] M.O. Amdur, J.C. Doulland, D. Classen, Casarett and Doull's toxicology, In: The Basic (Ed), Science of Poisons, Pergamon Press, New York, NY, (1991), 639–643.

[3] A. Mudipalli, Lead hepatotoxicity & potential health effects, Indian J. Med. Res. 126 (2006) 518–527.

[4] G. García-Rosales, A. Colín-Cruz, Biosorption of lead by maize (Zea mays) stalk sponge, J. Environ. Manage. 91 (2010) 2079–2086.

[5] X. Xiao, S.L. Luo, G.M. Zeng, W.Z. Wei, Y. Wan, L. Chen, H. J. Guo, Z. Cao, L.X. Yan, J.L. Chen, Q. Xi, Biosorption of cadmium by Endophytic Fungus (EF) *Microsphaeropsis* sp. LSE10 isolated from cadmium hyperaccumulator *Solanum Nigrum* L, Bioresour. Technol. 101(6) (2010) 1668–1674.

[6] S.L. Luo, L. Yuan, L.Y. Chai, X.B. Min, Y.Y. Wang, Y. Fang, P. Wang, Biosorption behaviors of Cu^{2+}, Zn^{2+}, Cd^{2+} and mixture by waste activated sludge, Trans. Nonferrous Metal Soc. China 16(6) (2006) 1431–1435.

[7] Y. He, G.M. Zhou, Research progress on excess sludge reduction technologies, Environ. Technol. 1 (2004) 39–42.

[8] X.B. Min, Y.Y. Wang, X. Yu, Study and development of activated sludge treatment of heavy metal containing wastewater, Indust. Water Wastewater 35(4) (2004) 9–11.

[9] C.R.T. Tarley, M.A.Z. Arruda, Biosorption of heavy metals using rice milling by-products: Characterisation and application for removal of metals from aqueous effluents, Chemosphere 54(7) (2004) 987–995.

[10] J.M. Luo, X. Xiao, S.L. Luo, Biosorption of cadmium(II) from aqueous solutions by industrial fungus *Rhizopus cohnii*, Trans. Nonferrous Met. Soc. China 20 (2010) 1104–1111.

[11] H. Yazid, R. Maachi, Biosorption of lead(II) ions from aqueous solutions by biological activated dates stems, J. Environ. Sci. Technol. 1(4) (2008) 201–213.

[12] H. Yazid, Z. Sadaoui, R. Maachi, Removal of cadmium (II) ions from aqueous phase by biosorption on biological activated dates' pedicels (kinetic, equilibrium and thermodynamic study), Inter. J. Chem. Rea. Eng. 9 (2011) A93.

[13] A. Namane, A. Hellal, The dynamic adsorption characteristics of phenol by granular activated carbon, J. Hazard. Mater. B137 (2006) 618–625.

[14] A.S. Michaels, Simplified method of interpreting kinetic data in fixedbed ion exchange, Ind. Eng. Chem. 44 (1952) 1922–1930.

[15] G.M. Lukchis, Adsorption system-design by mass transfer concept, Chem. Eng. 80 (1973) 111–116.

[16] S.K. Mishra, S.B. Kamumgo, R. Rajew, Adsorption of sodium dodecyl Benzensulfonates onto coal, J. Colloid Inter. Sci. 267 (2003) 42–48.

[17] M. Iqbal, A. Saeed, S.I. Zafar, FTIR spectrophotometry, kinetics and adsorption isotherms modeling, ion exchange, and EDX analysis for understanding the mechanism of Cd^{2+} and Pb^{2+} removal by mango peel waste, J. Hazard. Mater. 164 (2009) 161–171.

[18] M.N. Mohamad Ibrahim, W.S. Wan Ngah, M.S. Norliyana, W.R. Wan Daud, M. Rafatullah, O. Sulaiman, R. Hashim, A novel agricultural waste adsorbent for the removal of lead(II) ions from aqueous solutions, J. Hazard. Mater. 182 (2010) 377–385.

[19] X. Li, Y. Tang, X. Cao, D. Lu, F. Luo, W. Shao, Preparation and evaluation of orange peel cellulose adsorbents for effective removal of cadmium, zinc, cobalt and nickel, Colloids Surf. A: Physicochem. Eng. Aspects 317 (2008) 512–521.

[20] H. Mokaddem, Z. Sadaoui, N. Boukhelata, N. Azouaou, Y. Kaci, Removal of Cadmium from aqueous solution by polysaccharide produced from *Paenibacillus polymyxa*, J. Hazard. Mater. 172 (2009) 1150–1155.

[21] L. Jin-ming, X. Xiao, L. Sheng-lian, Biosorption of cadmium(II) from aqueous solutions by industrial fungus *Rhizopus cohnii*, Trans. Nonferrous Met. Soc. China 20 (2010) 1104–1111.

[22] N. Barka, M. Abdennouri, A. Boussaoud, M. EL Makhfouk, Biosorption characteristics of Cadmium(II) onto *Scolymus hispanicus* L as low-cost natural biosorbent, Desalination 258 (2010) 66–71.

[23] N. Azouaou, Z. Sadaoui, A. Djaafri, H. Mokaddem, Adsorption of cadmium from aqueous solution onto untreated coffee grounds: Equilibrium, kinetics and, thermodynamics, J. Hazard. Mater. 184 (2010) 126–134.

[24] M.M. Montazer-Rahmati, P. Rabbani, A. Abdolalia, A.R. Keshtkar, Kinetics and equilibrium studies on biosorption of cadmium, lead, and nickel ions from aqueous solutions by intact and chemically modified brown algae, J. Hazard. Mater. 185 (2011) 401–407.

[25] S. Qaiser, A.R. Saleemi, M. Umar, Biosorption of lead from aqueous solution by Ficus religiosa leaves: Batch and column study, J. Hazard. Mater. 166 (2009) 998–1005.

[26] S. Doyurum, A. Çelik, Pb(II) and Cd (II) removal from aqueous solutions by olive cake, J. Hazard. Mater. 138 (2006) 22–28.

[27] M.M.D. Zulkali, A.L. Ahmad, N.H. Norulakmal, Oryza sativa L. husk as heavy metal adsorbent: Optimization with lead as model solution, Bioresour. Technol. 97 (2006) 21–25.

[28] Q. Feng, Q. Lin, F. Gong, S. Sugita, M. Shoya, Adsorption of lead and mercury by rice husk ash, J. Colloid Interf. Sci. 278 (2004) 1–8.

[29] A. Kapoor, T. Viraragharan, R.D. Cullimore, Removal of heavy metals using the fungus *Aspergillus niger*, Bioresour. Technol. 70 (1999) 95–104.

[30] F. Pagnanelli, S. Mainelli, F. Veglio, L. Toro, Heavymetal removal by olive pomace. biosorbent characterization and equilibrium modelling, Chem. Eng. Sci. 58 (2003) 4709–4717.

[31] S.R. Shukla, R.S. Pai, Removal of Pb(II) from solution using cellulose containing materials, J. Chem. Technol. Biotechnol. 80 (2005) 176–183.

[32] S.S. Ahluwalia, D. Goyal, Removal of heavy metals by waste tea leaves from aqueous solution, Eng. Life Sci. 5 (2005) 158–162.